engineering proceedings

MDPI

Proceedings Paper

One-step synthesis of robust 2D Ti_3C_2-MXene/AuNPs nanocomposite by electrostatic self-assembly for (bio)sensing

Ayesha Zaheer [1], Tina D'Aponte[1], Zaheer Ud Din Babar[1,2], Raffaele Velotta[1], Bartolomeo Della Ventura[1*] and Vincenzo Iannotti[1,3]

[1] Department of Physics "E. Pancini", University of Naples Federico II, Via Cintia 26, 80126, Naples, Italy
[2] Scuola Superiore Meridionale (SSM), University of Naples Federico II, Largo S. Marcellino, 10, 80138, Italy
[3] CNR–SPIN (Institute for Superconductors, Oxides and Other Innovative Materials and Devices), Piazzale V. Tecchio 80, 80125 Naples, Italy
* Correspondence: Correspondence: bartolomeo.dellaventura@unina.it
† Presented at the 4th International Electronic Conference on Applied Sciences (Online), 27 Oct–10 Nov 2023

Abstract: In this study, we present a single-step approach for the synthesis of Ti_3C_2 MXene and gold nanoparticle (AuNP) composites via electrostatic self-assembly. The surface of the AuNPs was modified to induce a positive charge using cetyltrimethylammonium bromide (CTAB), which enabled effective electrostatic interactions with negatively charged MXene sheets. The successful synthesis of the MX-AuNP composite was confirmed using UV-Vis spectroscopy (UV-Vis), dynamic light scattering (DLS), and scanning electron microscopy (SEM). In conclusion, our single-step synthesis method offers a sustainable platform for producing MXene-AuNP composites with enhanced properties. This approach can be extended to other metal nanoparticles and holds great promise for a wide range of applications, particularly in biosensing and nanomaterial-based technologies.

Keywords: Ti_3C_2 MXene; gold nanoparticles; nanocomposite; MXene@AuNPs; electrostatic self-assembly

Citation: To be added by editorial staff during production.

Academic Editor: Manoj Gupta

Published: xx

1. Introduction

Recently, biosensing has emerged as a prominent and rapidly growing research area. The use of low-dimensional materials appears to be an effective strategy to meet the need for high-efficiency and sensitive biosensors with low detection limits. In this context, MXenes, two-dimensional carbides, and nitrides have garnered significant attention from the biosensing community owing to their exceptional features that are favorable for sensing [1,2]. MXenes are layered structures composed of carbides, nitrides, and carbonitrides produced from their parent MAX phase 3D precursors by eliminating interleaved A layers under carefully controlled etching [3]. In addition to their hydrophilicity, conductivity, and dispersibility, MXenes possess a unique structure with intrinsic functional groups, making them compatible to form composites with other metals [4]. Consequently, this can significantly enhance the detection efficiency of MXene-based sensing platforms. Ti_3C_2 MXene is a pioneering member in family of MXenes that proved it immense potential in biosensing [4], and many other promising research areas [5]. Gold nanoparticles (AuNPs) exhibit remarkable properties and have been widely employed in MXene research. Rakhi et al. [6] reported an amperometric biosensor for glucose sensing using a Ti_3C_2/Au nanocomposite, achieved through a chemical reduction approach to decorate MXene with Au clusters. Another study reported the synthesis of MXene hybrids with Au, Ag, and Pd nanoparticles via self-reduction of precursor salts [7]. Yang et al. [8] studied the synthesis of Nb_2C/Au composites via electrostatic self-assembly after modifying the MXene surface with APTES, resulting in excellent SERS performance. However, it is worth noting that

modification of the MXene surface with APTES and other polymers can affect its intrinsic conductivity. MXene can function as a reducing agent and reduce aqueous metal salts to nanoparticles. However, they are commonly used for noble metal nanoparticles. Additionally, the in-situ reduction of gold presents challenges in controlling the shape and size of AuNPs and requires facile control [9]. Therefore, designing a universal approach is crucial. Electrostatic self-assembly is a simple and highly efficient method for fabricating composites. Owing to their negative surface, MXenes can serve as an active platform to host oppositely charged particles. In the simple approach proposed by Xie et al., Au nanorods were deposited on $Ti_3C_2T_x$ nanosheets via electrostatic self-assembly [10]. However, there is a strong limitation to the size yield of nanorods, and controlling their size is difficult [11]. Thus, it is imperative to develop a robust and controllable method to prepare MXene-AuNP composites without using stabilizers, in situ reduction, or creating an intermediate matrix, such as APTES and polymers.

Spherical AuNPs produced using Turkevich protocols are highly regarded in this manner because of their facile synthesis, easy control, and high reproducibility [12]. To the best of our knowledge, a composite of MXene with spherical AuNPs via electrostatic self-assembly, while preserving the properties of MXene, has never been reported. Herein, we report a one-step synthesis of a Ti_3C_2 MXene/AuNP composite via electrostatic self-assembly. To achieve this, cetyltrimethylammonium bromide (CTAB) was utilized as a cationic surfactant to introduce a positive charge to gold nanoparticles (AuNPs) produced using the conventional Turkevich protocol [13]. The synergies between both materials can significantly enhance the properties of the composite, making it a promising candidate for various applications, particularly in biosensing.

2. Materials and Methods

2.1. Materials

Ti_3AlC_2 MAX precursor (Particle Size ≤ 40 μm) was acquired from Carbon-Ukraine. Hydrochloric acid (HCl, ≥ 37%, ACS reagents), Lithium Chloride (LiCl, 99%), gold (III) chloride trihydrate ($HAuCl_4{\cdot}3H_20$), Sodium Citrate, Ascorbic acid, Silver Nitrate, Cetyltrimethylammonium bromide (CTAB) were purchased from Sigma-Aldrich. Ethanol (≥ 99.5%) was obtained from Merck Millipore. Durapore ® 0.22μm, 47 mm PVDF hydrophobic membranes were used for vacuum filtration. Ultrapure deionized water was dispensed using a MilliQ system (18.2 MΩ cm resistivity) and used for all experiments.

2.2. Synthesis of MXene

MXene was synthesized via wet chemical etching route with modifications in protocols reported [14]. Ti_3AlC_2 MAX powder (1 g) was slowly added to a Nalgene bottle containing MilliQ water (9 ml), HCl (18 ml), and HF (3 ml). and continuously stirred for 24 h at 35 °C. The solution was thoroughly washed with MilliQ water by centrifugation at 4200 rpm for 5 min for each cycle until the pH reaches ~6-7. Delamination was performed in a solution of MilliQ + LiCl (50 mL + 1 g) at 35 °C for 24 h at 600 rpm under constant argon bubbling. The solution was subsequently washed until clay-like sediment appeared. The clay sediment was redispersed, hand-shaken, and centrifuged to obtain delaminated flakes. The delaminated flakes were washed repeatedly to ensure MXene quality and were stored at 4°C.

2.3. Synthesis of Positively charged Gold Nanoparticles

Gold nanoparticles (AuNPs) were synthesized using the classic Turkevich method with slight modifications [15]. Briefly, 0.5 ml (25.4 mM) of $HAuCl_4{\cdot}3H_2O$ was spiked in 50 ml MilliQ under vigorous magnetic stirring until boiling. Subsequently, 1 ml of sodium citrate (80 mM) was added with constant stirring for approximately 20 min while maintaining a constant temperature. The color of the solution first changed from yellowish to dark and finally to wine red. To remove citrate impurities, the solution was washed at

6000 rpm for 30 min, and the pellet was redispersed in ultrapure water (Milli-Q). The final AuNP solution was stored in a refrigerator (4 °C) in the dark.

Gold growth was initiated using a gold growth solution [16]. To this end, 0.384 mL of $HAuCl_4 \cdot 3H_2O$ (40 mM) was added to 6 ml CTAB (200 mM) under gentle stirring. The color of the suspension turned bright orange-yellow. Subsequently, 0.228 ml of $AgNO_3$ (10 mM) was added to control the gold growth process, ensuring the formation of spherical particles. Subsequently, 0.960 mL of ascorbic acid (100 mM) was added and the solution immediately turned colorless. Ascorbic acid acts as a weak reducing agent, causing the reduction of Au(III) to Au(0), as indicated by the colorless color change [17]. The solution was then diluted with 11 mL ultrapure water with gentle stirring for 20 min. Finally, Turkevich gold nanoparticles (AuNPs) were mixed with the growth solution. The solution appeared reddish-pink in color, indicating an increase in the nanoparticle size due to the surfactant. To remove the surfactant, the solution was washed twice with ultrapure water at 7000 rpm for 30 min, and the pellet was redispersed in water to reach an optical density (OD) of 1.0. CTAB serves a dual purpose: stabilizing the nanoparticles i.e. preventing aggregation, and controlling the growth and shape of the nanoparticles through the CTAB bilayer. These actions result in the introduction of a positive charge on the surface of the AuNPs through its quaternary ammonium head group. This charge modification is crucial for achieving well-dispersed positively charged spherical AuNPs that are suitable for electrostatic self-assembly.

2.4. Synthesis of MXene and Gold Nanoparticle Composite (MXene@AuNP)

The MXene/AuNP nanocomposite was synthesized via electrostatic self-assembly to decorate the $Ti_3C_2T_x$ MXene sheets with AuNPs. Briefly, 4 mL of an aqueous solution of AuNPs (7.15×10^{10} NPs/ml) was added dropwise to 4 mL of a colloidal solution of MXene (1 mg/mL) under gentle stirring at room temperature for 1 h. The samples were then centrifuged at 3500 rpm for 30 min to remove excess unbound AuNPs and the precipitate was redispersed in MilliQ water. The samples were sonicated for 30 min to ensure homogeneity. The resulting sample was denoted as MX@AuNPs.

3. Results and Discussion

UV-Vis. absorbance spectra were recorded on a UV/Vis spectrophotometer (model 6715 Jenway, Cole-Parmer® Company) with a resolution of 0.1 nm. Dynamic Light Scattering (DLS) measurements were conducted using a Zetasizer Nano ZS instrument (Malvern Instruments). The measurements were performed at 25°C with an equilibration time of 100 s. Prior to the analysis, the samples were homogenized by sonication, and each measurement was repeated three times. Zeta potential measurements were performed using the same instrument and the results were recorded as the mean value of the zeta potential ± standard deviation. The morphology of the MXene@AuNP composite was examined using a Zeiss ΣIGMA field-emission scanning electron microscope (FESEM).

3.1. MXene Synthesis and Delamination:

UV-Vis spectra were recorded for $Ti_3C_2T_x$ MXene, AuNP, and MXene@AuNPs composites. The colloidal solution of delaminated $Ti_3C_2T_x$ MXene (black line) exhibited a characteristic absorption peak at ~795 nm, as shown in Fig. 1a [18]. The inset shows that the MXene dispersion exhibits a typical greenish color, which signifies successful delamination [19].

3.2. AuNPs synthesis

The AuNPs displayed a peak at approximately 530 nm in the visible light region, corresponding to the surface plasmon resonance (SPR) of spherical Au nanoparticles (Figure 1d). The estimated size based on this SPR was 40-50 nm, which was consistent with the DLS results (Figure 1e).

3.3. MX@AuNPs Composite Synthesis

Zeta potential (ζ-potential) measurements were performed to confirm the electrostatic interactions between Ti_3C_2 MXene and AuNPs, ζ -potential measurements were performed as shown in Figure 1b. The mean zeta potential of MXene is -24 mV owing to the presence of negative surface terminations (− F, − OH) at neutral pH [20]. AuNPs showed a ζ-potential of +11 mV, indicating the possibility of electrostatic self-assembly. When positively charged spherical AuNPs come into proximity with negatively charged MXene nanosheets, they induce electrostatic interactions. These interactions led to the formation of the MXene/AuNP composite. The SEM image (Fig. 1c) shows uniform distribution of AuNPs across the MXene sheets without any noticeable agglomeration. Figure 1d shows the UV-visible spectra of AuNPs with a peak at ~529 nm in the visible light region. In contrast, the AuNP peak is evident with a typical MXene peak, indicative of MX@AuNPs composite formation. DLS studies suggested that the MXene sample had an average diameter of approximately 300 nm, representing small flakes dispersed in the solution (Figure 1e). This size reduction can also be attributed to the sonication performed during composite synthesis and before the measurements. An increase in the diameter of the flakes after loading MXenes with AuNPs was also observed. This can be ascribed to the electrostatic interactions between oppositely charged species, which lead to an increase in the hydrodynamic size and signify composite formation.

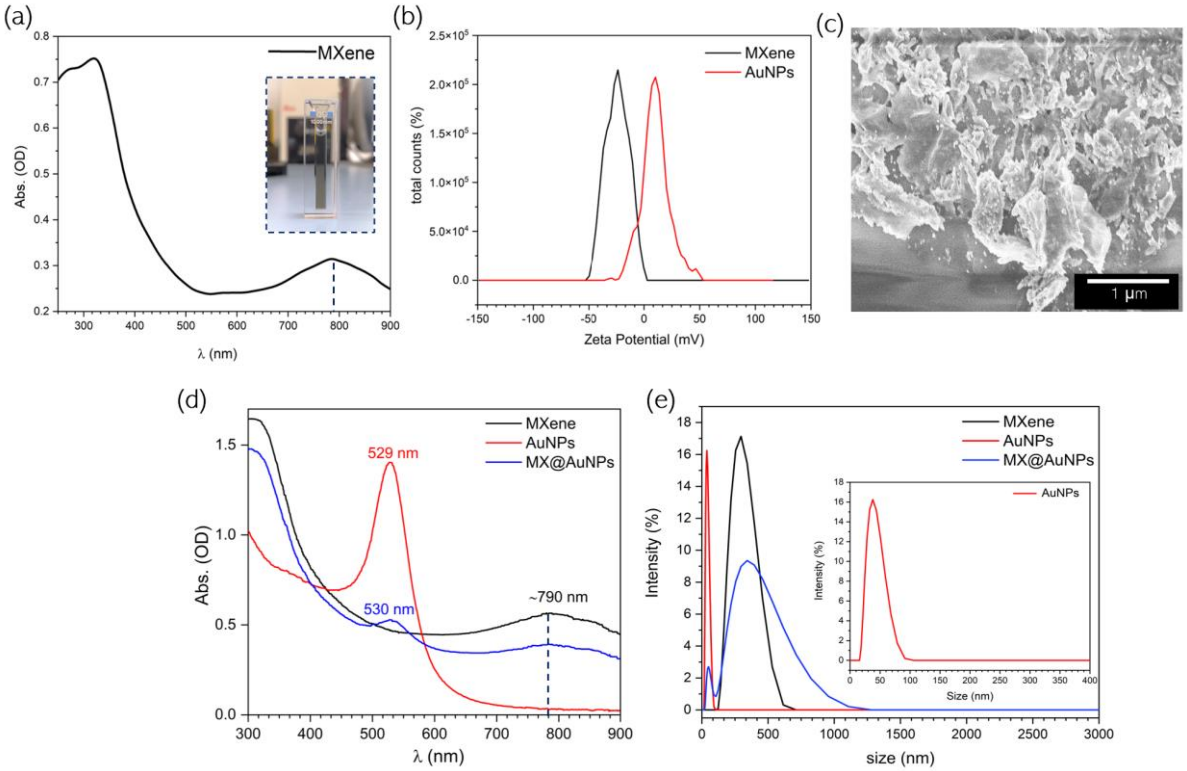

Figure 1. (a) UV-visible spectra of freshly delaminated Ti_3C_2 MXenes depicting their standard spectra. **(b)** Zeta potential of $Ti_3C_2T_x$ MXene (black) and AuNPs (red) with contrasting polarities, thus showing compatibility with electrostatic binding. **(c)** SEM micrograph of MXene@AuNPs composite showing AuNP decorated over the MXene sheets **(d)** UV-visible spectra of spherical MXene, AuNPs, and colloidal solution of MX@AuNPs composite **(e)** DLS analysis of MXene, AuNPs, and MX@AuNPs.

3. Conclusions:

This paper presents a single-step approach for the synthesis of Ti_3C_2 MXene and surface-charged modified Turkevich gold nanoparticle (AuNP) composites via electrostatic self-assembly. Ti_3C_2 MXene was produced via HF+HCL approach and delaminated by Li-

ions Intercalation. Delamination yields high-quality MXene single flakes with a significantly negative zeta potential (-24 mV), allowing them to be uniformly dispersed in water. Cetyltrimethylammonium bromide (CTAB) induces a positive core around the AuNPs (ζ-potential = +11 mV), thus enabling effective electrostatic interactions with the negatively charged surface of the MXene sheets. The UV-visible spectra confirmed the delamination of MXene. UV-visible spectra, DLS measurements, and SEM images showed the successful dispersion of AuNPs over the MXene sheets. In conclusion, our preliminary studies suggest a single-step method as a quick and sustainable approach for producing MXenes@AuNPs composites. This approach can be extended to other nanomaterials, and holds great promise for a wide range of applications, particularly in biosensing.

Supplementary Materials: Not Applicable

Author Contributions: Conceptualization: B.D.V., R.A., and V.I.; methodology, B.D.V., A.Z. T. D. A. and Z. U. D. B., resources, R.V. and V.I.; data curation. Z.U.B.D, A.Z., R.V., V.I.; writing—original draft preparation, A.Z., Z.U.D.B.; writing—review and editing, Z.U.B.D., A.Z., B.D.V.; supervision, B.D.V.; project administration, R.V., V.I.; Funding acquisition, R.V. and V.I. All the authors have read and agreed to the published version of the manuscript.

Funding: This research received no external funding.

Institutional Review Board Statement: Not Applicable

Informed Consent Statement: Not Applicable

Data Availability Statement: Not Applicable

Conflicts of Interest: The authors declare no conflict of interest.

References

1. Gogotsi, Y.; Huang, Q. MXenes: Two-Dimensional Building Blocks for Future Materials and Devices. *ACS Nano* **2021**, *15*, 5775-5780, doi:10.1021/acsnano.1c03161.
2. Ho, D.H.; Choi, Y.Y.; Jo, S.B.; Myoung, J.-M.; Cho, J.H. Sensing with MXenes: Progress and Prospects. **2021**, *33*, 2005846, doi:https://doi.org/10.1002/adma.202005846.
3. Lim, K.R.G.; Shekhirev, M.; Wyatt, B.C.; Anasori, B.; Gogotsi, Y.; Seh, Z.W. Fundamentals of MXene synthesis. *Nature Synthesis* **2022**, *1*, 601-614, doi:10.1038/s44160-022-00104-6.
4. Babar, Z.U.D.; Della Ventura, B.; Velotta, R.; Iannotti, V. Advances and emerging challenges in MXenes and their nanocomposites for biosensing applications. *RSC Adv* **2022**, *12*, 19590-19610, doi:10.1039/d2ra02985e.
5. Maleki, A.; Ghomi, M.; Nikfarjam, N.; Akbari, M.; Sharifi, E.; Shahbazi, M.-A.; Kermanian, M.; Seyedhamzeh, M.; Nazarzadeh Zare, E.; Mehrali, M.; et al. Biomedical Applications of MXene-Integrated Composites: Regenerative Medicine, Infection Therapy, Cancer Treatment, and Biosensing. **2022**, *32*, 2203430, doi:https://doi.org/10.1002/adfm.202203430.
6. Rakhi, R.B.; Nayak, P.; Xia, C.; Alshareef, H.N. Novel amperometric glucose biosensor based on MXene nanocomposite. *Scientific Reports* **2016**, *6*, 36422, doi:10.1038/srep36422.
7. Satheeshkumar, E.; Makaryan, T.; Melikyan, A.; Minassian, H.; Gogotsi, Y.; Yoshimura, M. One-step Solution Processing of Ag, Au and Pd@MXene Hybrids for SERS. *Scientific Reports* **2016**, *6*, 32049, doi:10.1038/srep32049.
8. Yang, Z.; Jiang, L.; Zhao, W.; Shi, B.; Qu, X.; Zheng, Y.; Zhou, P. Nb2C MXene self-assembled Au nanoparticles simultaneously based on electromagnetic enhancement and charge transfer for surface enhanced Raman scattering. *Spectrochimica Acta Part A: Molecular and Biomolecular Spectroscopy* **2023**, *299*, 122843, doi:https://doi.org/10.1016/j.saa.2023.122843.
9. Li, K.; Jiao, T.; Xing, R.; Zou, G.; Zhou, J.; Zhang, L.; Peng, Q. Fabrication of tunable hierarchical MXene@AuNPs nanocomposites constructed by self-reduction reactions with enhanced catalytic performances. *Science China Materials* **2018**, *61*, 728-736, doi:10.1007/s40843-017-9196-8.
10. Xie, H.; Li, P.; Shao, J.; Huang, H.; Chen, Y.; Jiang, Z.; Chu, P.K.; Yu, X.-F. Electrostatic Self-Assembly of Ti3C2Tx MXene and Gold Nanorods as an Efficient Surface-Enhanced Raman Scattering Platform for Reliable and High-Sensitivity Determination of Organic Pollutants. *ACS Sensors* **2019**, *4*, 2303-2310, doi:10.1021/acssensors.9b00778.

11. Scarabelli, L.; Sánchez-Iglesias, A.; Pérez-Juste, J.; Liz-Marzán, L.M. A "Tips and Tricks" Practical Guide to the Synthesis of Gold Nanorods. *The Journal of Physical Chemistry Letters* **2015**, *6*, 4270-4279, doi:10.1021/acs.jpclett.5b02123.
12. Wuithschick, M.; Birnbaum, A.; Witte, S.; Sztucki, M.; Vainio, U.; Pinna, N.; Rademann, K.; Emmerling, F.; Kraehnert, R.; Polte, J. Turkevich in New Robes: Key Questions Answered for the Most Common Gold Nanoparticle Synthesis. *ACS Nano* **2015**, *9*, 7052-7071, doi:10.1021/acsnano.5b01579.
13. Khan, Z.; Singh, T.; Hussain, J.I.; Hashmi, A.A. Au(III)–CTAB reduction by ascorbic acid: Preparation and characterization of gold nanoparticles. *Colloids and Surfaces B: Biointerfaces* **2013**, *104*, 11-17, doi:https://doi.org/10.1016/j.colsurfb.2012.11.017.
14. Uzun, S.; Schelling, M.; Hantanasirisakul, K.; Mathis, T.S.; Askeland, R.; Dion, G.; Gogotsi, Y. Additive-Free Aqueous MXene Inks for Thermal Inkjet Printing on Textiles. **2021**, *17*, 2006376, doi:https://doi.org/10.1002/smll.202006376.
15. Turkevich, J.; Stevenson, P.C.; Hillier, J. A study of the nucleation and growth processes in the synthesis of colloidal gold. *Discussions of the Faraday Society* **1951**, *11*, 55-75, doi:10.1039/DF9511100055.
16. Sau, T.K.; Murphy, C.J. Seeded High Yield Synthesis of Short Au Nanorods in Aqueous Solution. *Langmuir* **2004**, *20*, 6414-6420, doi:10.1021/la049463z.
17. Nikoobakht, B.; El-Sayed, M.A. Preparation and Growth Mechanism of Gold Nanorods (NRs) Using Seed-Mediated Growth Method. *Chemistry of Materials* **2003**, *15*, 1957-1962, doi:10.1021/cm020732l.
18. Shuck, C.E.; Sarycheva, A.; Anayee, M.; Levitt, A.; Zhu, Y.; Uzun, S.; Balitskiy, V.; Zahorodna, V.; Gogotsi, O.; Gogotsi, Y. Scalable Synthesis of Ti3C2Tx MXene. **2020**, *22*, 1901241, doi:https://doi.org/10.1002/adem.201901241.
19. Shekhirev, M.; Shuck, C.E.; Sarycheva, A.; Gogotsi, Y. Characterization of MXenes at every step, from their precursors to single flakes and assembled films. *Progress in Materials Science* **2021**, *120*, 100757, doi:https://doi.org/10.1016/j.pmatsci.2020.100757.
20. Ying, Y.; Liu, Y.; Wang, X.; Mao, Y.; Cao, W.; Hu, P.; Peng, X. Two-Dimensional Titanium Carbide for Efficiently Reductive Removal of Highly Toxic Chromium(VI) from Water. *ACS Applied Materials & Interfaces* **2015**, *7*, 1795-1803, doi:10.1021/am5074722.